Astron. Astrophys. 324, 877–887 (1997)

ASTRONOMY
AND
ASTROPHYSICS

Short 21-cm WSRT observations of spiral and irregular galaxies

H I properties

A.H. Broeils[1] **and M.-H. Rhee**[2]

[1] Stockholm Observatory, S-13336 Saltsjöbaden, Sweden
[2] Kapteyn Astronomical Institute, Postbus 800, 9700 AV Groningen, The Netherlands

Received 13 May 1996 / Accepted 15 January 1997

Abstract. We present the analysis of neutral hydrogen properties of 108 galaxies, based on short 21-cm observations with the Westerbork Synthesis Radio Telescope (WSRT). The results of two H I surveys are analysed to investigate the existence of relations between optical and H I properties, like diameters, hydrogen masses and average surface densities. For all galaxies in our sample we find that the H I diameter, defined at a surface density level of 1 $M_\odot$ pc^{-2}, is larger than the optical diameter, defined at the 25$^{\rm th}$ mag arcsec^{-2} isophotal level. The H I-to-optical-diameter ratio does not depend on morphological type or luminosity. The strongest, physically meaningful, correlation for the sample of 108 galaxies is the one between log $M_{\rm HI}$ and log $D_{\rm HI}$, with a slope of 2. This implies that the H I surface density averaged over the whole H I disc is constant from galaxy to galaxy, independent of luminosity or type. The radial H I surface density profiles are studied using the technique of principal component analysis. We find that about 81 % of the variation in the density profiles of galaxies can be explained by two dimensions. The most dominant component can be related to "scale" and the second principal component accounts for the variance in the behaviour of the radial profile in the central parts of galaxies (i.e. "peak or depression") . The third component accounts for 7 % of the variation and is most likely responsible for bumps and wiggles in the observed density profiles.

Key words: galaxies: fundamental parameters – galaxies: structure – galaxies: kinematics and dynamics – galaxies: spiral – radio lines: galaxies

1. Introduction

Two H I surveys of spiral and irregular galaxies have been performed by means of short observations in the 21-cm line of neutral hydrogen with the Westerbork Synthesis Radio Telescope (WSRT). They provide one-dimensional information about the kinematics and distribution of the neutral hydrogen gas projected on the so-called resolution axis. The observations of each galaxy were made in such a way that the resolution axis coincides with the major axis of that galaxy, so that a position-velocity map (XV-map) of the H I distribution projected on the major axis was obtained. From these maps global H I profiles and H I strip integrals, $\Sigma_{\rm HI}(x)$, representing the projections of the entire neutral hydrogen distributions on the major axes, were derived. Subsequently these data were used to estimate for each galaxy a number of H I properties, like H I flux, H I mass, systemic velocity, global profile widths, and isophotal diameter of the hydrogen disc. The results have been published in Broeils & van Woerden (1994, hereafter Paper I) and Rhee & van Albada (1996, hereafter Paper II).

In the present paper these properties are analysed and combined with optical information on the sample galaxies. Because many studies of the integral properties (including neutral hydrogen) of larger and more complete samples have been published (e.g. Roberts 1969; Shostak 1978; Huchtmeier & Richter 1988; Roberts & Haynes 1994, hereafter RH), we will concentrate our attention on the specific characteristics of our data: spatial information on the H I distribution of an intermediate-sized sample of galaxies. The analysis of the kinematics (H I linewidths, rotation velocities and the Tully-Fisher relation) is discussed in an accompanying paper (Rhee & Broeils 1996).

In Sect. 2 we will investigate correlations between H I and optical properties, like morphological type, luminosity and optical diameter. We will show that the H I diameter correlates well with the optical size of a galaxy and also with the total neutral hydrogen mass. The latter correlation indicates that the average H I surface density per galaxy is constant to first order. Possible dependences of this quantity on morphological type and luminosity will also be investigated. Furthermore, the total mass of each galaxy inside the H I diameter is determined and correlated with optical properties. The edge of the H I distribution is generally the outermost point of the mass distribution of a galaxy that can be measured. The total mass defined within this point is therefore the best galaxy mass estimator that we have for an intermediate-sized sample of galaxies. In the second part

Send offprint requests to: A.H. Broeils

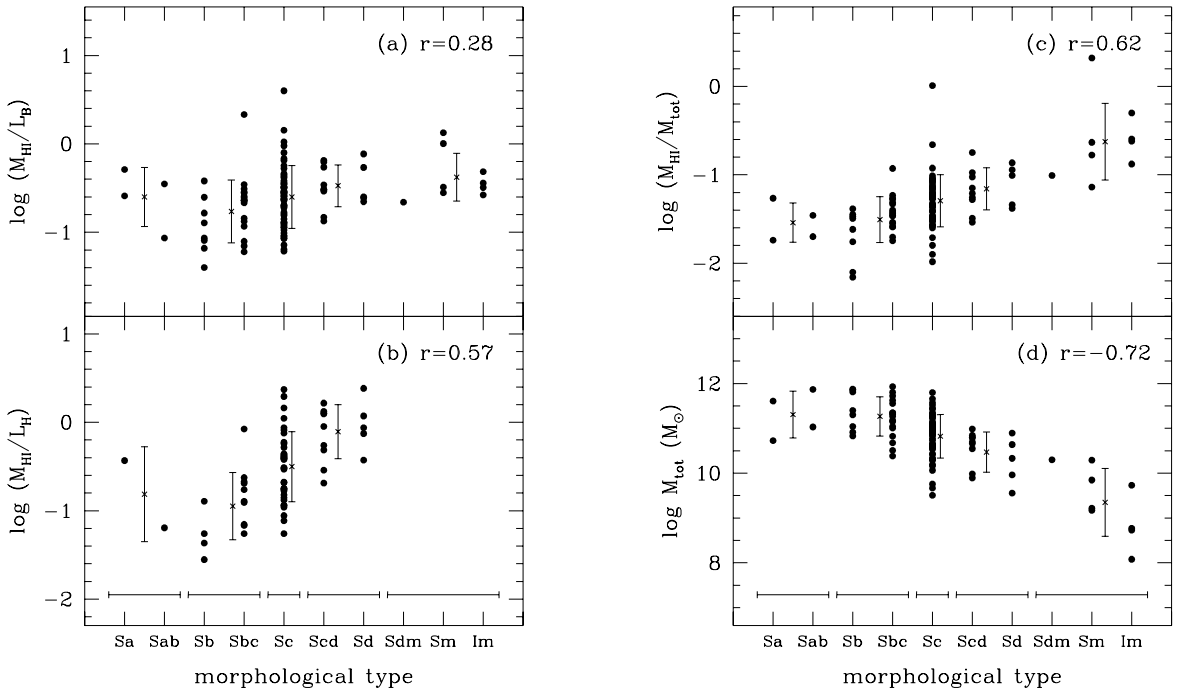

Fig. 1a–d. Dependences on morphological type of the hydrogen-mass-to-B-luminosity ratio (**a**), the hydrogen-mass-to-H-luminosity ratio (**b**), the H I-to-total-mass ratio (**c**), and the total mass (**d**). In each plot the linear correlation coefficient r is given. The correlation with total mass is the strongest relation with morphological type for our sample. Comparison of panel (**c**) with (**a**) and (**b**) shows that the increase of gas fraction with type is more prominent when normalized by total mass than by luminosity of a galaxy

of this paper (Sect. 3) we will study the radial H I surface density distributions of the sample galaxies by means of Principal Component Analysis (PCA). It has been shown (Paper I; Cayatte et al. 1994) that although H I density profiles show quite some diversity, when they are normalized by a certain radius scale and averaged per morphological type, there seems to exist a characteristic profile for each morphological type. PCA will be used to investigate how many independent dimensions (principal components) are required to explain the observed variance in the H I surface density distributions and we will try to link these components to actual physical parameters.

2. Global H I properties

Since the pioneering work by Roberts (1969), who investigated integral properties of a sample of about 100 galaxies, many studies have been published describing correlations between H I and optical properties (e.g. Shostak 1978; Huchtmeier & Richter 1988; RH). Several relations between H I content, morphological type and other global parameters were established. These studies involved large samples of galaxies (typically more than 100), observed with single-dish radio telescopes. On the other hand, synthesis observations of galaxies were made to compare the distributions of gas and light in detail (e.g. Bosma 1978, 1981; Wevers 1984; Broeils 1992). The sample sizes used in these synthesis studies are in general small, on the order of 10-20 galaxies.

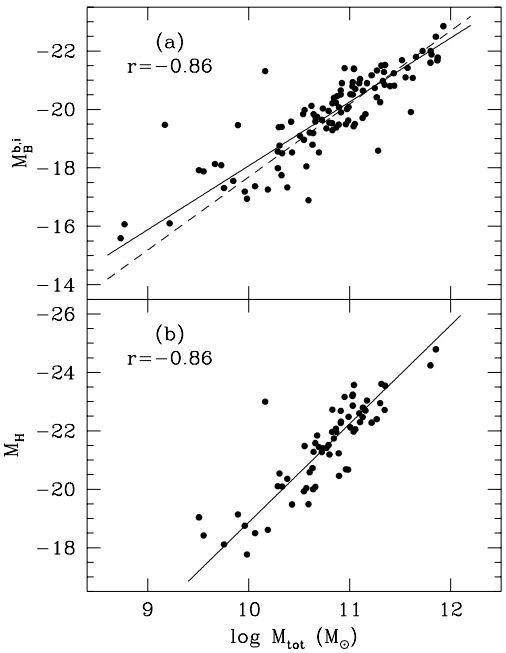

Fig. 2a and b. Correlations between total enclosed mass inside the H I radius and the blue (**a**), and near-infrared (**b**) absolute magnitudes. The solid lines show the least-squares fit to all the data points; the dashed line indicates the relation for constant $M_{\rm tot}/{\rm L_B} = 5.4\,{\rm M}_\odot/{\rm L_{B_\odot}}$, which is consistent with the data for galaxies with $M_{\rm tot} > 10^{10}\,{\rm M}_\odot$

The type of H I data analysed in this paper contains more spatial information than provided by single-dish observations, but less than provided by *usual* synthesis observations. Also the sample size (108 galaxies) lies between those of single-dish and synthesis studies. In this paper we therefore concentrate on properties that are special to these two surveys: radial H I surface density profiles, average surface densities and sizes of hydrogen discs.

The reader should keep in mind that certain correlations might be biased by the way the sample was defined. The details of the selection criteria can be found in Papers I and II, and their significance for the correlations are discussed in Sect 2.4. The properties of the sample are listed in Table 1[1].

2.1. H I and total mass

The traditional method to normalize and compare the H I content of galaxies is to use the distance-independent parameter $M_{\rm HI}/L_{\rm B}$. It has been shown that this ratio depends on morphological type (Roberts 1969; Shostak 1978; RH) in the sense that later types have larger $M_{\rm HI}/L_{\rm B}$ ratios. For the galaxies in our sample this is also the case (see Fig. 1a), but the correlation is rather weak, maybe as a result of the inherent bias to this sample, that only gas-rich galaxies were selected (see Papers I and II). The average value and standard deviation of the $M_{\rm HI}/L_{\rm B}$ ratio are $0.36 \pm 0.47\,{\rm M}_\odot/{\rm L}_{\rm B_\odot}$. By analogy to the situation concerning the Tully-Fisher relation, one might expect a tighter correlation between gas content and morphological type by using infrared magnitudes, since the latter suffer less from absorption and reddening effects. Bothun (1984) has shown that the type dependence is somewhat stronger if one scales the gas content to $H_{0.5}$ magnitudes (i.e. the H magnitude measured within an aperture of one-third of the blue diameter, from Aaronson et al. 1982), but that within a given morphological bin the range in $M_{\rm HI}/L_{\rm H_{0.5}}$ is as large as in the blue band. This is confirmed by our Figs. 1a and b. The average value and standard deviation of the $M_{\rm HI}/L_{\rm H_{0.5}}$ ratio are $0.51 \pm 0.55\,{\rm M}_\odot/{\rm L}_{\rm H_\odot}$.

An alternative way to compare the H I contents of galaxies is to normalize the H I masses by the total masses. Assuming a spherical mass distribution, the total mass can be computed by $M_{\rm tot} = 0.5\,V^2\,D/G$. For V we take the maximum rotation velocity, $V_{\rm max}$ (column 12 of Table 1), determined from the XV-maps (see Broeils 1992 and Paper II). Usually, the optical diameter (e.g. de Vaucouleurs or Holmberg diameter, see Faber & Gallagher 1979) is used to define $M_{\rm tot}$, since the optical radius is approximately the outermost point where visible, galaxian material is detected. Because we can detect neutral hydrogen far beyond the optical boundaries, we use the H I diameter, defined at a surface density level of $1\,{\rm M}_\odot\,{\rm pc}^{-2}$, to estimate the total enclosed mass. The mass thus derived can be considered as an upper limit to the mass *enclosed* inside the H I radius, because in most cases $V_{\rm max}$ is somewhat larger than the rotation velocity of the last measured point of the rotation curve, and because a spherical mass distribution is used. Of course, the true total mass of a galaxy will even be larger, since there is no evidence that the outer edge of the mass distribution has been reached with the H I observations. In other words, *the masses thus derived are the best determined lower total-mass limits presently available for an intermediate-size galaxy sample.* In Fig. 1c the ratio of H I to total mass is plotted as a function of morphological type. It shows that late-type galaxies have much larger $M_{\rm HI}/M_{\rm tot}$ ratios than the classical spirals. This correlation is much stronger than the $M_{\rm HI}/L_{\rm B}$ versus type relation shown in Fig. 1a, but its usefulness as "H I measuring tool" is limited by the fact that the ratio is distance-dependent. Not only the hydrogen-to-total-mass ratio correlates well with morphological type, but also the total mass itself is strongly type-dependent as is shown in Fig. 1d. With a correlation coefficient of $r = -0.72$ it correlates more strongly with type than for example $M_{\rm HI}$ ($r = -0.48$) or blue luminosity $L_{\rm B}$ ($r = -0.60$) do. The pronounced decrease for the dwarf systems might be somewhat exaggerated, due to the intrinsic difficulties of determining total masses for systems with narrow, Gaussian-shaped global H I profiles (Broeils 1992).

In Fig. 2 the plots of the total mass $M_{\rm tot}$ versus absolute blue magnitude $M_{\rm B}^{\rm b,i}$ and absolute near infrared magnitude $M_{\rm H}$ are shown. The least-squares fits of these data, indicated by the solid lines, are

$$\begin{aligned} M_{\rm B}^{\rm b,i} &= (-2.19 \pm 0.12)\ \log M_{\rm tot}\ + (3.80 \pm 1.28)\ , \\ M_{\rm H} &= (-3.37 \pm 0.21)\ \log M_{\rm tot}\ + (14.86 \pm 2.30)\ , \end{aligned} \qquad (1)$$

with $r = -0.86$ and a dispersion of 0.81 mag for the blue band, and $r = -0.86$ and 0.83 mag for the near infrared H band. For the blue band, the slope is considerably smaller than -2.5, the value found in earlier studies by e.g. Shostak (1978) and Huchtmeier & Richter (1988). A linear term with a slope of -2.5 in Eq.(1) would indicate that the total mass-to-light ratio $M_{\rm tot}/{\rm L}_{\rm B}$ of spirals would be constant. If we consider only galaxies with $\log M_{\rm tot} > 10$, then a constant $M_{\rm tot}/{\rm L}_{\rm B}$ of $5.4\,{\rm M}_\odot/{\rm L}_{\rm B_\odot}$ ($M_{\rm B}^{\rm b,i} = -2.5 \log M_{\rm tot} + 7.31$), indicated by the dashed line in Fig. 2, is indeed consistent with the data points. The total-mass-to-light ratios of low-mass galaxies in our sample seem to be systematically smaller, possibly due to underestimations of the total masses for these galaxies as mentioned above. For the H band this effect is not visible, mainly because of the lack of H band data for dwarf galaxies. If a constant mass-to-light ratio is in any way related to the physics behind the existence of a Tully-Fisher relation (as is usually assumed), then Fig. 2 tells us that one should be careful with the inclusion of low-luminosity dwarf galaxies in the application of the Tully-Fisher relation.

2.2. H I diameters

There is a strong correlation between the (angular) H I diameter $D_{\rm HI}$, defined at a surface density of $1\,{\rm M}_\odot\,{\rm pc}^{-2}$ and the optical absorption-corrected diameter $D_{25}^{\rm b,i}$, measured at the $25^{\rm th}$mag arcsec^{-2} isophote:

$$\log D_{\rm HI} = (1.00 \pm 0.03) \log D_{25}^{\rm b,i} + (0.23 \pm 0.04)\ , \qquad (2)$$

[1] All optical properties, i.e. magnitudes and diameters, were taken from the LEDA database. Since the optical properties in paper I are largely based on the RC2 (de Vaucouleurs et al. 1976), small differences between paper I and this paper might exist.

Table 1. Properties of the sample galaxies.

Name	Type	$D_{\rm HI}$ kpc	$D_{25}^{\rm b,i}$ kpc	$R_{\rm eff}$ kpc	$M_{\rm HI}$ $10^{10}{\rm M}_\odot$	$M_{\rm tot}$ $10^{10}{\rm M}_\odot$	$M_{\rm HI}/L_{\rm B}^{\rm b,i}$ $\frac{{\rm M}_\odot}{{\rm L}_{{\rm B}_\odot}}$	$M_{\rm HI}/L_{\rm H}$ $\frac{{\rm M}_\odot}{{\rm L}_{{\rm H}_\odot}}$	$M_{\rm HI}/M_{\rm tot}$	$\langle\sigma_{\rm HI}\rangle$ $\frac{{\rm M}_\odot}{{\rm pc}^2}$	$V_{\rm max}$ km/s
(1)	(2)	(3)	(4)	(5)	(6)	(7)	(8)	(9)	(10)	(11)	(12)
D 77	SBdm	24	18	8	0.20	1.99	0.22		0.10	4.31	84
D 80	SBm	33	31	10	0.31	0.15	0.32		2.09	3.62	20
D 105	SBm	31	21	11	0.33	1.94	1.34		0.17	4.32	73
D 165	Im	5	3	2	0.01	0.01	0.32		0.50	3.06	14
D 168	IBm	8	3	2	0.02	0.06	0.36		0.25	2.98	25
D 185[a]	SBm	8	5	2	0.01	0.16	0.28		0.07	2.39	42
I 167	SBc	55	32	18	0.92	4.19	0.53		0.22	3.86	81
I 381	SBbc	56	29	14	0.81	14.83	0.23	0.20	0.05	3.33	151
I 529	Sc	48	34	14	0.79	12.68	0.20	0.39	0.06	4.44	151
N 100	Sc	33	14	11	0.20	3.73	0.79	0.82	0.05	2.34	98
N 514	SBc	47	36	14	0.72	21.31	0.19		0.03	4.11	197
N 691	Sbc	43	36	16	0.44	27.43	0.09		0.02	2.97	233
N 697	SBc	76	45	21	2.12	37.43	0.37		0.06	4.69	206
N 753	Sbc	106	51	36	2.41	63.44	0.24		0.04	2.73	227
N 772	Sb	91	70	31	2.55	71.50	0.16	0.13	0.04	3.96	261
N 784	SBd	14	8	4	0.05	0.36	0.22	0.87	0.14	3.18	47
N 803	Sc	41	23	11	0.62	7.33	0.32	0.38	0.08	4.64	124
N 818	Sc	59	45	29	1.77	33.05	0.24		0.05	6.47	219
N 918	SBc	32	21	10	0.26	7.38	0.29	0.17	0.03	3.10	140
N 949	Sc	15	9	5	0.06	2.02	0.12	0.15	0.03	3.26	106
N 1003	Scd	69	18	15	0.60	9.68	0.55	1.33	0.06	1.59	110
N 1156	IBm	13	8	3	0.07	0.54	0.26		0.13	5.35	60
N 1171	Sc	58	30	17	0.82	10.66	0.25	0.18	0.08	3.12	126
N 1560	Sd	17	7	5	0.09	0.91	0.77	1.18	0.10	3.97	68
N 2268	Sbc	47	33	12	0.44	22.47	0.07	0.07	0.02	2.55	203
N 2357	Sc	53	24	16	0.42	13.45	0.35	0.18	0.03	1.90	148
N 2460	Sa	68	18	22	0.74	40.41	0.51		0.02	2.02	226
N 2535	Sc	74	37	25	1.49	1.46	0.29	0.39	1.02	3.47	41
N 2541	Scd	34	18	10	0.37	3.52	0.62	1.65	0.11	4.11	94
N 2683	Sb	18	13	7	0.06	8.20	0.04	0.03	0.01	2.24	198
N 2715	Sc	40	24	14	0.33	8.38	0.09		0.04	2.61	134
N 2742	Sc	27	18	9	0.20	7.54	0.09		0.03	3.53	155
N 2770	Sc	42	25	11	0.70	11.38	0.24	0.44	0.06	4.99	152
N 2976	Sc	7	6	2	0.01	0.32	0.06	0.14	0.04	3.64	63
N 2998	Sc	102	51	41	2.17	45.50	0.27		0.05	2.66	196
N 3027	Sd	58	22	15	0.89	7.86	0.54	2.42	0.11	3.39	108
N 3041	SBc	35	22	9	0.25	9.41	0.16		0.03	2.70	153
N 3254	Sbc	42	25	13	0.52	18.54	0.23	0.24	0.03	3.81	195
N 3264	SBcd	20	13	7	0.14	0.78	0.15	1.27	0.18	4.46	58
N 3319	SBcd	32	20	10	0.32	4.58	0.30	1.25	0.07	4.03	111
N 3338	Sc	63	33	18	1.20	22.19	0.36	0.41	0.05	3.91	175
N 3359	SBc	74	37	20	1.49	16.53	0.32	0.75	0.09	3.46	139
N 3432	SBd	25	13	8	0.18	4.35	0.25	0.75	0.04	3.69	122
N 3486	Sc	26	16	8	0.22	6.76	0.28		0.03	4.24	149
N 3614	Sc	57	47	21	1.30	17.74	0.43		0.07	5.09	164
N 3646	Sbc	97	60	28	3.09	84.82	0.14		0.04	4.18	274
N 3666	SBc	30	16	9	0.27	5.88	0.32	0.30	0.05	3.81	130
N 3675	Sb	32	22	11	0.16	20.09	0.08	0.04	0.01	1.98	232
N 3733	Sc	53	26	18	0.66	9.18	0.68	1.46	0.07	2.99	122
N 3756	Sbc	39	25	13	0.30	10.14	0.12	0.17	0.03	2.47	149
N 3769	SBbc	20	8	6	0.16	3.22	0.23		0.05	4.90	117

Table 1. (continued)

Name	Type	$D_{\rm HI}$ kpc	$D_{25}^{\rm b,i}$ kpc	$R_{\rm eff}$ kpc	$M_{\rm HI}$ $10^{10}{\rm M}_\odot$	$M_{\rm tot}$ $10^{10}{\rm M}_\odot$	$M_{\rm HI}/L_{\rm B}^{\rm b,i}$ $\frac{\rm M_\odot}{\rm L_{B_\odot}}$	$M_{\rm HI}/L_{\rm H}$ $\frac{\rm M_\odot}{\rm L_{H_\odot}}$	$M_{\rm HI}/M_{\rm tot}$	$\langle\sigma_{\rm HI}\rangle$ $\frac{\rm M_\odot}{\rm pc^2}$	$V_{\rm max}$ km/s
(1)	(2)	(3)	(4)	(5)	(6)	(7)	(8)	(9)	(10)	(11)	(12)
N 3877	Sc	27	19	8	0.16	8.16	0.06	0.06	0.02	2.78	161
N 3893	Sc	48	21	14	0.55	12.45	0.16	0.21	0.04	3.05	149
N 3917	Scd	33	20	10	0.20	6.19	0.13	0.21	0.03	2.33	127
N 3949	Sc	18	11	5	0.20	3.58	0.13	0.21	0.06	8.05	132
N 3953	SBbc	38	35	13	0.37	20.58	0.06	0.06	0.02	3.26	216
N 4062	Sc	17	10	5	0.05	4.29	0.11	0.11	0.01	2.38	147
N 4068	Im	6	4	2	0.01	0.05	0.48		0.24	4.60	28
N 4096	Sc	22	14	6	0.13	4.39	0.10	0.17	0.03	3.47	131
N 4100	Sc	40	25	14	0.37	13.56	0.13	0.12	0.03	2.86	170
N 4144	SBc	8	6	2	0.02	0.57	0.17	0.52	0.04	4.49	79
N 4157	SBbc	36	19	9	0.37	14.34	0.28	0.13	0.03	3.57	184
N 4183	Sc	31	15	9	0.25	4.01	0.33	0.60	0.06	3.20	105
N 4217	Sab	27	22	9	0.22	10.75	0.09	0.06	0.02	3.90	187
N 4414	Sc	20	9	6	0.11	10.96	0.13	0.08	0.01	3.56	216
N 4534	Sc	25	9	7	0.19	2.11	0.95		0.09	3.97	86
N 4545	SBc	44	28	12	0.58	8.16	0.20	0.29	0.07	3.81	126
N 4559	Scd	46	26	13	0.66	6.98	0.29	0.55	0.09	3.97	114
N 4605	SBc	7	6	2	0.02	0.46	0.07		0.04	5.20	76
N 4814	Sb	57	36	16	0.81	25.13	0.25		0.03	3.23	196
N 4861	SBm	24	13	8	0.16	0.70	1.01		0.23	3.63	50
N 5023	Sc	15	7	4	0.05	1.16	0.38	0.87	0.05	3.08	82
N 5205	Sbc	32	25	12	0.31	6.70	0.31	0.21	0.05	3.82	134
N 5350	SBbc	67	34	16	0.92	35.76	0.21		0.03	2.62	215
N 5351	SBbc	61	40	17	1.28	21.88	0.25		0.06	4.44	176
N 5523	Scd	33	20	10	0.35	6.32	0.34	0.49	0.06	4.10	128
N 5529	Sc	83	53	26	1.59	63.13	0.23	0.13	0.03	2.95	256
N 5533	Sab	114	48	37	2.57	73.92	0.35		0.03	2.52	236
N 5678	SBb	28	26	8	0.37	11.00	0.07		0.03	6.13	184
N 5783	SBc	46	29	15	0.64	11.27	0.65		0.06	3.86	145
N 5879	Sbc	25	15	8	0.16	4.77	0.13	0.12	0.03	3.34	128
N 5894	SBc	26	23	10	0.42	10.74	0.11	0.09	0.04	7.64	187
N 5899	SBc	44	33	16	0.60	18.65	0.11		0.03	4.02	192
N 5951	SBc	32	22	9	0.37	5.44	0.23	0.42	0.07	4.49	120
N 5985	Sb	78	56	24	1.13	64.70	0.13		0.02	2.36	267
N 6207	Sc	23	12	6	0.19	3.46	0.14		0.05	4.49	113
N 6236	SBc	24	18	7	0.25	2.12	0.28		0.12	5.55	87
N 6255	SBc	22	15	7	0.17	2.69	0.41	1.11	0.06	4.31	102
N 6339	SBc	33	26	11	0.32	4.57	0.26	0.31	0.07	3.65	109
N 6643	Sc	31	26	9	0.49	8.91	0.09	0.11	0.06	6.68	158
N 6674	SBb	125	60	42	3.07	74.55	0.38		0.04	2.50	226
N 6689	SBc	20	12	6	0.11	1.94	0.28	0.43	0.06	3.52	91
N 6690	Sd	21	12	7	0.10	2.14	0.25	0.37	0.05	2.83	94
N 7177	SBb	22	17	7	0.16	6.74	0.09	0.06	0.02	4.14	161
N 7497	SBc	52	26	14	0.95	9.77	0.57	0.40	0.10	4.54	128
N 7664	Sc	69	35	21	1.51	27.67	0.46		0.05	4.00	185
N 7741	SBc	23	17	6	0.21	2.63	0.20		0.08	5.26	100
N 7753	SBbc	105	58	35	2.80	52.81	0.28		0.05	3.22	208
N 7817	Sbc	34	27	13	0.44	11.04	0.08	0.07	0.04	4.90	168
U 2855	Sc	41	28	11	0.61	19.13	1.43		0.03	4.60	200
U 3137	Sbc	26	14	9	0.28	2.41	2.15	0.84	0.12	5.54	90
U 3580	Sa	43	20	14	0.29	5.30	0.26	0.37	0.05	1.98	103

Table 1. (continued)

Name	Type	$D_{\rm HI}$	$D_{25}^{\rm b,i}$	$R_{\rm eff}$	$M_{\rm HI}$	$M_{\rm tot}$	$M_{\rm HI}/L_{\rm B}^{\rm b,i}$	$M_{\rm HI}/L_{\rm H}$	$M_{\rm HI}/M_{\rm tot}$	$\langle\sigma_{\rm HI}\rangle$	$V_{\rm max}$
		kpc	kpc	kpc	$10^{10}{\rm M}_\odot$	$10^{10}{\rm M}_\odot$	$\frac{\rm M_\odot}{\rm L_{B_\odot}}$	$\frac{\rm M_\odot}{\rm L_{H_\odot}}$		$\frac{\rm M_\odot}{\rm pc^2}$	km/s
(1)	(2)	(3)	(4)	(5)	(6)	(7)	(8)	(9)	(10)	(11)	(12)
U 5459	SBc	39	19	11	0.43	7.80	0.45	0.57	0.06	3.69	132
U 7699	SBcd	10	6	3	0.03	0.96	0.30	0.90	0.03	3.57	91
U 8146	Sc	21	9	7	0.13	1.55	1.05	1.96	0.09	3.70	79
U 11635	Sbc	73	54	26	1.46	42.21	0.35		0.03	3.48	223
U 11651	Scd	31	20	9	0.26	4.96	0.65	0.29	0.05	3.37	117
U 11707	Sc	32	17	10	0.35	3.91	3.99	2.35	0.09	4.43	103

Notes:

Column 3: H I diameter defined by a surface density of 1 $M_\odot{\rm pc}^{-2}$.

Column 4: Optical diameter defined at the 25$^{\rm th}$ mag arcsec^{-2} isophote and corrected for Galactic and internal extinctions following Tully & Fouqué (1985).

Column 5: H I effective radius, enclosing 50 % of the H I mass.

Column 6: Total H I mass.

Column 7: Total mass enclosed inside the H I diameter $D_{\rm HI}$ (see text).

Column 8: H I-mass-to-blue-luminosity ratio. The total blue luminosity has been corrected for Galactic and internal extinctions following Tully & Fouqué (1985).

Column 9: H I-mass-to-near-infrared-luminosity ratio. The near-infrared luminosity has been taken from Tormen & Burstein (1995), which has been corrected for Galactic extinction

Column 10 : H I-mass-to-total-mass ratio.

Column 11 : Mean value of the H I surface density, averaged over the whole H I disc (see text).

Column 12 : Maximum rotation velocity.

[a] The heliocentric velocity of DDO 185 in paper I was mistakenly listed as 373 km/s. It should be 140 km/s. The adopted distance (and all the distance-dependent parameters) will remain the same, since they are based on membership in the M 101 group.

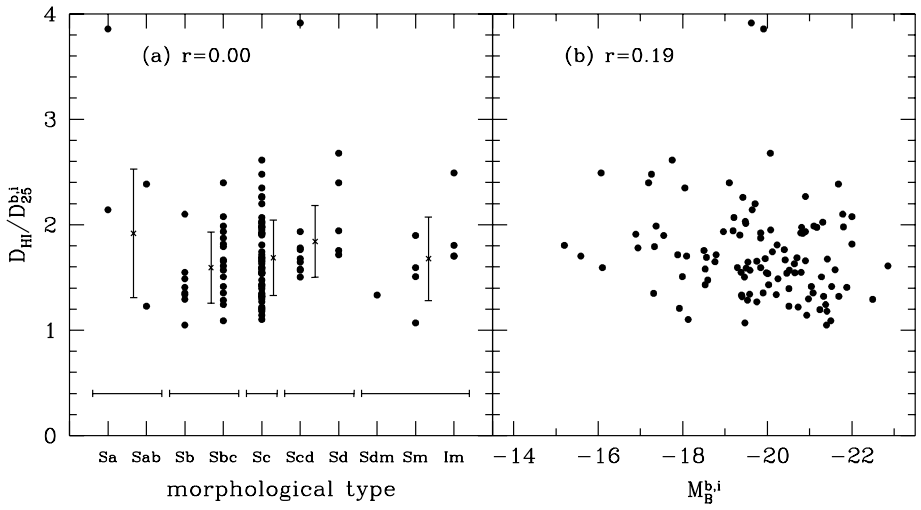

Fig. 3a and b. Ratio of H I and optical diameters, $D_{\rm HI}/D_{25}^{\rm b,i}$, as a function of morphological type (**a**) and luminosity (**b**). The crosses with error bars in panel (**a**) show the average values and 1σ dispersions obtained by averaging the data in bins indicated by the horizontal bars. The correlation coefficients are shown in the upper left corner of each panel. Two galaxies (NGC 2460 and NGC 1003) with $D_{\rm HI}/D_{25}^{\rm b,i}$ greater than 3 have been excluded from calculation of average values

with a linear correlation coefficient of r = 0.93, implying that the distance-independent diameter ratio $D_{\rm HI}/D_{25}^{\rm b,i}$ is constant. The average value is $D_{\rm HI}/D_{25}^{\rm b,i}$ = 1.7$\pm$0.5. In Fig. 3, we plot this ratio versus morphological type (a) and luminosity (b). Fig. 3a shows no obvious correlation of the diameter ratio with type. The type dependence of the diameter ratio has been discussed before by Bosma (1981), Giovanelli & Haynes (1983), Wevers (1984) and Warmels (1986), amongst others, on the basis of smaller samples. More recently, Cayatte et al. (1994) constructed a sample of 84 galaxies with H I diameter information with types ranging from S0 to Im. (This sample has a considerable overlap with the sample analysed here, since it contains 39 out of the 48 galaxies in the sample of paper I.) These studies find a weak correlation of diameter ratio with type, in the sense that the average $D_{\rm HI}/D_{25}^{\rm b,i}$ ratio is lower for early types. Given the width of the diameter ratio distribution per type and the relatively small number of Sa, Sab galaxies in our sample, we can not confirm these results. Fig. 3b indicates that a weak trend between the diameter ratio and absolute luminosity might exist:

low luminosity galaxies seem to have slightly larger $D_{\rm HI}/D_{25}^{\rm b,i}$ than more luminous galaxies.

Fig. 3 further shows that for all galaxies the size of the neutral hydrogen disc is larger than that of the optical disc. Selection effects might play a role here, since there is a strong correlation between the linear H I diameter and H I mass, as shown in Fig. 4 by the filled circles (with r = 0.98 this is actually the strongest correlation between two physically meaningful parameters for our sample); by selecting galaxies with sufficient H I flux, we have selected against galaxies with small H I diameters. As shown already by Shostak (1978), the H I mass also correlates strongly with the optical diameter with almost the same slope as that of $M_{\rm HI}$ versus $D_{\rm HI}$. For our sample the relation between $M_{\rm HI}$ and $D_{25}^{\rm b,i}$ is shown by the open circles in Fig. 4. Since both relations run parallel for our sample, a flux limited sample will always contain galaxies that have diameter ratios larger than 1, if the relations shown in Fig. 4 hold for all galaxies. The least-squares fits to these data, indicated by the two lines, are

$$\log M_{\rm HI} = (1.96 \pm 0.04)\ \log D_{\rm HI} + (6.52 \pm 0.06)\ ,$$
$$\log M_{\rm HI} = (1.95 \pm 0.06)\ \log D_{25}^{\rm b,i} + (7.00 \pm 0.08)\ , \qquad (3)$$

with r = 0.98 and a dispersion of 0.13 dex for the $M_{\rm HI} - D_{\rm HI}$, and r = 0.94 and 0.19 dex for the $M_{\rm HI} - D_{25}^{\rm b,i}$ relation. Use of $R_{\rm eff}$ (the radius enclosing 50% of the H I mass, see paper II) instead of $D_{\rm HI}$ gives basically the same result as $R_{\rm eff}$ and $D_{\rm HI}$ are tightly correlated (r = 0.99). It is interesting to note that the effective radius coincides with the optical radius ($\langle R_{25}^{\rm b,i}/R_{\rm eff}\rangle$ = 1.0 ± 0.2), which means that on average there are equal amounts of gas inside and outside the optical edge of a galaxy.

2.3. Mean H I surface density

The tight correlation between $\log M_{\rm HI}$ and $\log D_{\rm HI}$, with a slope close to 2, implies a nearly constant mean H I surface density, averaged over the whole H I disc. This parameter, $\langle\sigma_{\rm HI}\rangle = 4M_{\rm HI}/\pi {D_{\rm HI}}^2$, is not correlated with either morphological type or luminosity, as shown in Fig. 5. Only galaxies of types Sa/Sab seem to have somewhat lower average surface densities. The small variation of the mean H I density among the late-type spirals and dwarf irregular systems has been demonstrated before (Bottinelli 1971, Huchtmeier & Richter 1988, and most clearly by RH) using the hybrid H I surface density, $\langle\sigma^*_{\rm HI}\rangle$ defined as the total H I mass divided by the *optical* surface area inside R_{25}. The scatter of the distribution is however much smaller for $\langle\sigma_{\rm HI}\rangle$ than for the hybrid density $\langle\sigma^*_{\rm HI}\rangle$. The mean values and standard deviations are $3.8 \pm 1.1\ {\rm M}_\odot\ {\rm pc}^{-2}$ and $11.2 \pm 5.3\ {\rm M}_\odot\ {\rm pc}^{-2}$, respectively.

2.4. Selection biases

The above correlations might be biased by the way the galaxies were selected in the first place. The most important selection criteria were: (a) large H I contents, (b) optical diameters greater than 3′, and (c) inclinations greater than 40°. In particular criterion (a) has to be taken into account in judging the H I properties

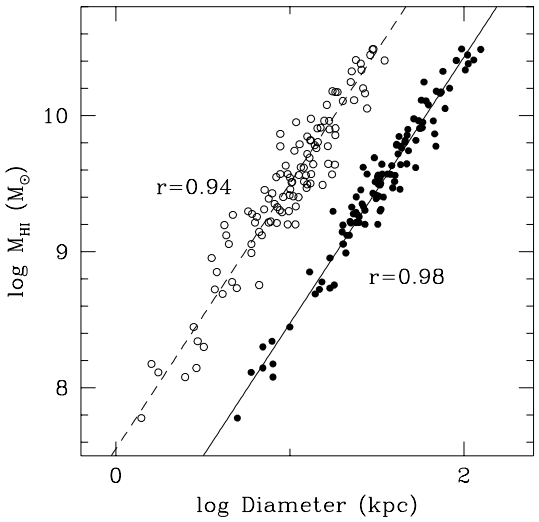

Fig. 4. Correlation between H I mass and linear H I diameter (filled circles) and linear optical diameter (open circles). The open circles were shifted by 0.3 in the logarithm to the left-hand side of the diagram to separate them from the other points. The straight lines represent the results of least-squares fits, which both have slopes of about 2. This implies a nearly constant H I surface density when averaged over the whole disc. Note that the scatter for the H I diameters is significantly smaller than for the optical diameters

of this sample. In this section we discuss this by comparing our results with those from Roberts & Haynes (1994, RH), Kamphuis, Sijbring & van Albada (1996), and de Blok, McGaugh & van der Hulst (1996).

RH discussed the quantifiable properties of galaxies and their dependence on morphological type based on objects that are included both in the RC3 and in the Uppsala General Catalogue (Nilson 1973; UGC) with additional H I line data from the so-called Arecibo General Catalog (AGC) maintained by R. Giovanelli and M. Haynes. Comparison of Figs. 1 and 5a with those of RH show good agreement both in terms of absolute values and the dependence on morphological type. Note however that in at least three of the four panels in Fig. 1 the Sa/Sab galaxies do not seem to agree with the correlations found for the other types. They generally seem to have an H I content that is too high compared to the other types. RH showed that the distribution of H I masses and densities of Sa/Sab galaxies is substantially wider than those of late-type spirals. Our early-type spirals are clearly not representative for their type, but selected for their known high H I content.

Kamphuis et al. (1996) obtained short WSRT observations (similar to ours) for a sample of 57 galaxies without prior H I information in the RC3. They show that the $M_{\rm HI}/L_{\rm B}$ ratios for the 42 detected galaxies agree well with the values obtained by RH (and therefore also with ours) with a slightly lower average value for the later types. de Blok et al. (1996) present VLA and WSRT H I data on 19 late-type low surface brightness (LSB) galaxies. They show that at a fixed luminosity these LSB have typically three times more H I than "normal" (HSB) galaxies,

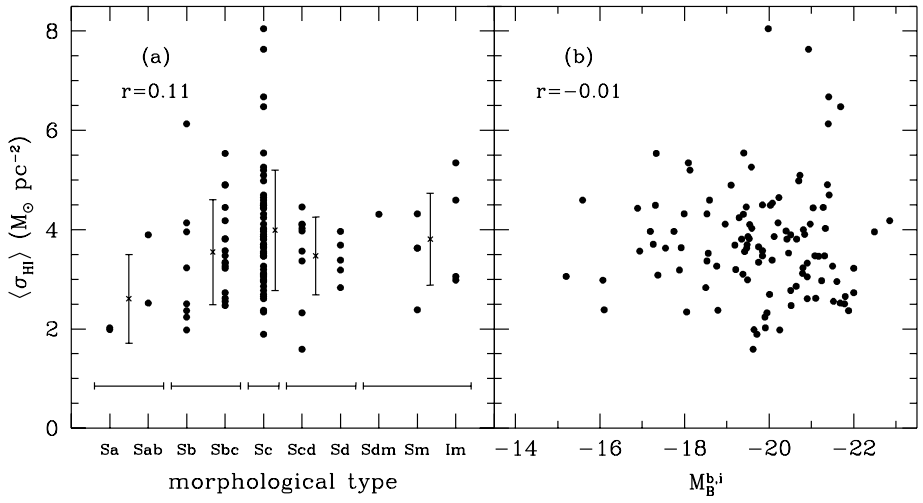

Fig. 5a and b. True H I surface density, averaged over the whole H I disc, $\langle\sigma_{\rm HI}\rangle$, as a function of morphological type (**a**) and luminosity (**b**). It shows a very weak correlation in the sense that late-type spirals have a slightly larger $\langle\sigma_{\rm HI}\rangle$ than early-types. The crosses indicate the average values calculated for the bins indicated by the horizontal bars

and that the H I surface density is about three times lower than those of HSB galaxies.

These comparisons indicate that by selecting galaxies with known H I properties we did not preferentially select the upper envelope of a wider distribution of H I masses for *normal* galaxies, but that the true distribution of H I content and densities might have a larger dispersion due to the properties of LSB galaxies. This does however apply to almost all published galaxy catalogs, since LSB galaxies are rarely included.

3. H I radial surface density distribution

So far the H I surface density distributions have only been used to define the sizes of the H I discs (e.g. $D_{\rm HI}$ and $R_{\rm eff}$; see Table 1), but these distributions themselves are of interest as well. For our sample they show a considerable diversity. When normalized by a certain radius scale (e.g. optical radius R_{25} as is usually done) and averaged per morphological type, there seems to exist a characteristic profile for each morphological type (see Figs. 7 and 8 in Paper I; see also Cayatte et al. 1994), although there is a significant scatter about the mean profile. The Sb-Sc galaxies tend to have very similar H I density profiles: more or less flat up to around R_{25}, and a steep drop beyond that point (Broeils & van Woerden 1994; Sancisi 1983). The Sd or later type galaxies mostly have density profiles that keep increasing towards the central parts (see e.g. Paper I). Early type galaxies (S0, Sa, Sab) are not well represented in the present sample; however, it is generally believed that these galaxies have central H I depressions (e.g. van Driel 1987; Sancisi 1983) and that the hydrogen gas might have an external origin.

In this paper we will take the analysis one step further: Principal Component Analysis (PCA) is used to investigate systematics of the H I radial surface density distributions. PCA is a statistical method which focuses on inter-object correlations, reduces their (parameter-space) dimensionality, and consequently finds the least number of the new dimensions (principal components) (see Murtagh & Heck 1987). Traditionally, the PCA method has often been used to find the most significant components among various global parameters (e.g. Whitmore 1984). Recently, Han (1995) has applied PCA to find the most important components in the surface brightness distributions of the spiral galaxies. He found that about 94 % of the variation in the surface brightness distribution of galaxies can be accounted for by just two principal components. In this paper we follow Han's line of approach to study the H I surface density distributions.

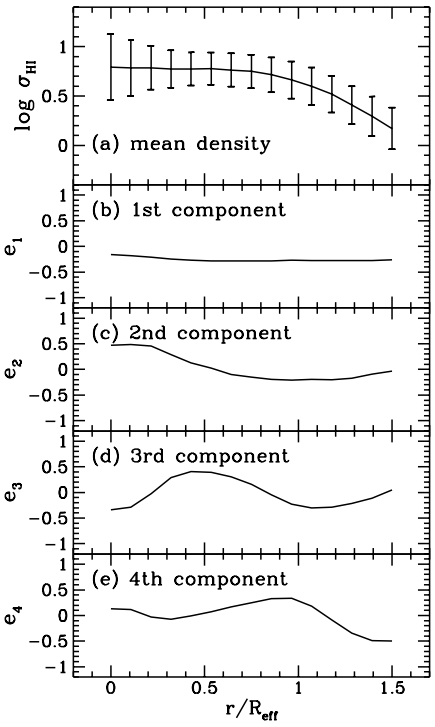

Fig. 6. a Mean H I surface density of the sample galaxies in units of $M_\odot$ pc^{-2}. Vertical error bars indicate 1σ of the H I surface density at the corresponding sampling points. **b**-**e** The first four principal components as a function of the H I effective radius $R_{\rm eff}$

In constructing the input dataset, we start with scaling the radii of the galaxies by $R_{\rm eff}$. In order to avoid that all data points

Table 2. Results of the Principal Component Analysis: eigenvalues (λ_j) for the first ten principal components.

j	λ_j	%	$\Sigma\lambda_j/15$ %
(1)	(2)	(3)	(4)
1	9.713	64.8	64.8
2	2.429	16.2	81.0
3	1.018	6.8	87.8
4	0.812	5.4	93.2
5	0.437	2.9	96.1
6	0.219	1.5	97.6
7	0.163	1.1	98.7
8	0.084	0.6	99.3
9	0.039	0.3	99.6
10	0.034	0.2	99.8

converge into one point ($\sigma_{\rm HI}$ = 1M$_\odot$ pc^{-2} at 1$D_{\rm HI}$), we choose $R_{\rm eff}$ for the scaling radius instead of $D_{\rm HI}$. We choose 15 sampling radii, from 0 to 1.5 $R_{\rm eff}$, with equal intervals in linear scale. This sampling roughly corresponds to one beam size on the major axes of typical galaxies in our sample. The H I surface densities of each galaxy (in linear scale) are then sampled at these radii. The 15 points represent the H I surface density distributions of the sample galaxies at the common scaled radii and PCA is expected to find the most important components in the H I distribution of galaxies. We have tested with different numbers, ranges and intervals of sampling points without finding significant differences. Neither does the use of logarithmic scaling of the H I surface densities change the results significantly.

In deriving the H I surface density distribution from the H I strip integrals, we have used an iterative deprojection method developed by Warmels (1986), with the assumptions of azimuthally symmetric distribution of H I, and constant inclination throughout the gas and stellar discs. Any violation of these assumptions, among other things, would increase the uncertainty in the H I density profile, and consequently, increase the dimensionality of the dataset studied in this paper. The possible existence of non-linear relations between the parameters could therefore lead to overestimation of some weak components.

Applying PCA to our input dataset produces a series of principal components (eigen vectors): The mean H I surface density profile and the first four principal components are presented in Fig. 6. First of all, the mean H I surface density profile shows a *shoulder* typical of Sb-Sc galaxies (Sancisi 1983) extending to about $R_{\rm eff}$, which coincides with the optical radius R_{25}. Note that our data sample is heavily biased towards Sc galaxies. Fig. 6b further shows that the first principal component has small variation in amplitude with radius and no change in sign. This implies that the most important physical process for the H I surface density profile works in a similar way at all positions within the galaxies. The first principal component is found to carry about 65 % of the total variance as listed in Table 2. The second principal component accounts for about 16 % of the total variance. It shows different behaviours for the inner and outer

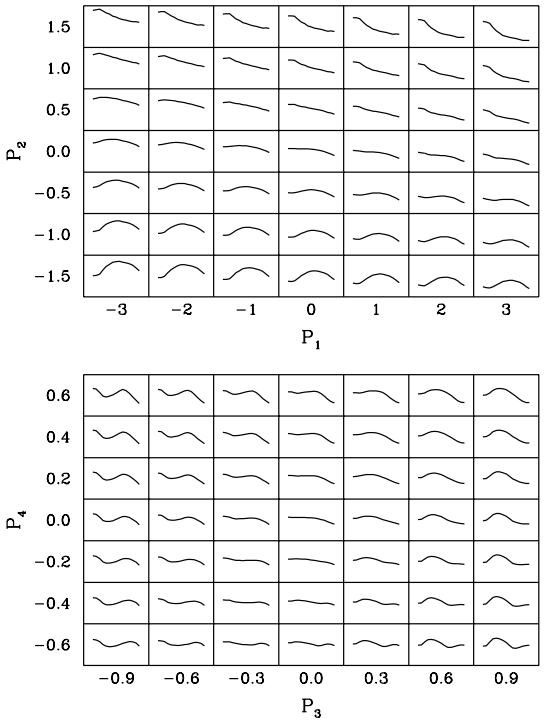

Fig. 7. (Top) Variations of the H I surface density profiles in the projection-plane of the first two principal components. The scale of the X-axis of each small panel is from -0.3 to 1.8 $R_{\rm eff}$ and the Y-axis from -1.3 to 2.4 log $\sigma_{\rm HI}$ in M$_\odot$ pc^{-2}. (Bottom) Variations of the HI surface density profiles in the projection-plane of the third and fourth principal components, setting P_1 and P_2 equal to zero

parts: Its sign changes around 0.5 $R_{\rm eff}$ from positive to negative and beyond around 0.5 $R_{\rm eff}$ it changes slowly with radius, staying negative. This component mainly determines the degree of depression (or boost) in the central part (see Fig. 7). The third component is found to explain about 7 % of the total variance. This component might be responsible for the wiggles and bumps in the H I surface density profile. It is possible that this component is related to the existence of the H I rings, bars or spiral-like structures. The fourth component accounts for 5 % of the total variance. It is not clear whether this component reflects weak but true features of the galaxies or just show random noise.

Therefore, at least three principal components are needed to account for about 90 % of the total variance, meaning that three (see Table 2) physical parameters mainly determine the shape of the H I radial surface density profiles. In Fig. 7, the variations of the H I radial surface density profiles are presented in the $P_1 - P_2$ and $P_3 - P_4$ planes. The principal component parameters P_1, P_2, P_3 and P_4 indicate the strength of the first, second, third and fourth principal components, respectively. The role of each principal component is better visible in these diagrams. Fig. 7 also shows that the shape of the HI surface density profiles can be parameterized by the principal components. Therefore, potentially, certain combinations of the principal component parameters could yield a good objective classification system for the H I surface density profiles. Furthermore, it could offer a better tool

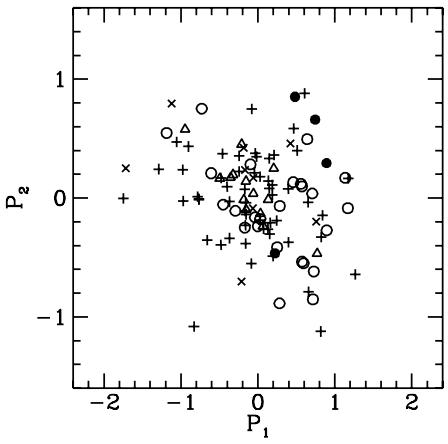

Fig. 8. Distribution of the sample galaxies in the $P_1 - P_2$ plane. The galaxies are grouped by the morphological type: the filled circles represents Sa, Sab galaxies, the open circles Sb, Sbc, the plus signs Sc, the open triangles Scd, Sd, and the crosses Sdm, Sm & Im

for the comparison of H I surface density profiles between field and cluster galaxies (cf. Cayatte et al. 1994). An asymmetry parameter can be defined by measuring the principal component parameters separately for the receding and approaching sides of a galaxy.

The question naturally arises whether the principal components are correlated with other parameters. The morphological dependence of the mean shape of the H I surface density profiles (see above discussions) is confirmed in Fig. 8 except for the Sa, Sab galaxies (the filled circle).

We have also examined the principal component parameters of the galaxies grouped by the presence of *optical* bar and ring structures. Mean differences in the principal component parameters are marginal for the galaxies with and without bars. In the $P_3 - P_4$ plane ringed galaxies tend to shift toward the upper-left direction from the origin, where non-ringed galaxies are located. It would be interesting to investigate whether the principal component parameters show more prominent differences between the galaxies with and without H I bar and ring structures, but two-dimensional information on the distribution of H I is needed to do this.

We also compared the principal component parameters and their simple combinations (e.g. $P_1 + P_2$, $P_1 - P_3$, and so on) of the sample galaxies with any of the global galaxian parameters listed in Table 1 and others from LEDA (IRAS far-infrared fluxes and colours), and with their combinations. In general, the principal component parameters do not show tight correlations with global parameters. The first principal component parameter shows some trend, though weak, with the maximum rotation velocity and H I diameter. It seems to correlate better with the (optical, far infrared and H I) mean surface brightness parameters and colours (U-B and B-V), but the correlations are weak at best. The second principal component does not show any trend with other global parameters. The third principal component shows a very weak trend with the optical (B band) mean surface brightness parameter. Combinations of the principal component parameters also tend to correlate better with the mean surface brightness parameters or colours.

4. Conclusions

In this paper a study of the neutral hydrogen properties of a sample of 108 galaxies, based on short 21-cm observations with the WSRT, has been presented. The observations, described in Papers I and II, provide one-dimensional information on the kinematics and spatial distribution of the neutral hydrogen along the major axis of each galaxy in the form of a position-velocity (XV) map. The kinematics will be discussed in an accompanying paper (Rhee & Broeils 1996). From these maps a number of H I properties were derived, like H I fluxes and masses, radial H I surface density profiles, and isophotal diameters of the H I discs.

In the first part of this paper these properties were correlated with the optical properties of the underlying galaxies, like luminosities, morphological type and an optical diameter. The main results are:

- The H I diameter ($D_{\rm HI}$), measured at a surface density level of $1 M_\odot\,{\rm pc}^{-2}$, correlates strongly with the (inclination- and absorption-corrected) optical diameter ($D_{25}^{\rm b,i}$), defined at the $25^{\rm th}$ mag arcsec^{-2} isophotal level. The diameter ratio, $D_{\rm HI}/D_{25}^{\rm b,i}$, shows no dependence on type or luminosity; the average value is $\langle D_{\rm HI}/D_{25}^{\rm b,i}\rangle = 1.7 \pm 0.5$. None of the galaxies in our sample has an H I disc smaller than the stellar disc.
- The average H I surface density $\langle\sigma_{\rm HI}\rangle$, defined by $\langle\sigma_{\rm HI}\rangle = 4\,M_{\rm HI}/\pi\,{D_{\rm HI}}^2$, hardly varies from galaxy to galaxy, although the H I masses vary by more than a factor 400. The average value is $3.8 \pm 1.1\,M_\odot\,{\rm pc}^{-2}$. The $\langle\sigma_{\rm HI}\rangle$'s of early-type spirals in our sample are only slightly smaller than the average value for the whole sample, probably due to the fact that these galaxies were selected for their H I-richness.
- The $M_{\rm HI}/L_{\rm B}$ ratio shows no correlation with luminosity, and only a weak correlation with type, maybe partly due to the above-mentioned selection effect. The $M_{\rm HI}/M_{\rm tot}$ mass ratio is more strongly correlated with morphological type, in the sense that this ratio increases for later types. This indicates that the neutral gas component becomes dynamically more important in late-type, gas-rich galaxies, which is confirmed by detailed mass models based on two-dimensional 21-cm synthesis observations (e.g. Carignan & Freeman 1985, Lake et al. 1990, Côté et al. 1991, Broeils 1992).
- The total mass inside $D_{\rm HI}$ correlates strongly with the morphological type of a galaxy, more strongly than H I mass or blue luminosity versus type. The strong correlation between total mass and luminosity is expected to be the basis of the small scatter in the Tully-Fisher relationship between luminosity and rotation velocity. The global mass-to-light ratios in the blue band ($M_{\rm tot}/L_{\rm B}^{\rm b,i}$) for the dwarf galaxies in our sample are slightly smaller than those for the more luminous galaxies. This indicates that one has to be careful with the use of dwarf galaxies in the Tully-Fisher relation.

The second part of this paper described a Principal Component Analysis of the radial H I density distributions of the sample galaxies. We showed that $\sim$ 81 % of the variations among surface density profiles can be accounted for by just two principal components. The first, dominant component is clearly linked to the "scale"; it has the same sign at all radii. In other words, the process that is linked to this component works in such a way that if it makes the surface density higher at one point it makes it higher at all other points. The second component is linked to the behaviour of the density profile in the central regions: peak or depression. The third component, which still accounts for 7 % of the variation, is most likely responsible for bumps and wiggles in the observed density profiles and could be linked to the presence of H I arms and rings. This could be confirmed by performing PCA to a large sample of galaxies with full two-dimensional synthesis observations of the neutral hydrogen distribution.

Acknowledgements. We would like to thank T.S. van Albada for his stimulation to start this project and H. van Woerden for his comments on the manuscript. We also thank the anonymous referee for useful suggestions. This research has made use of the LEDA database which is maintained by the Observatoire de Lyon and Observatoire de Paris-Meudon. We are grateful to the Netherlands Foundation for Research in Astronomy (ASTRON) and the Netherlands Organization for Scientific Research (NWO) for their support. AHB wishes to thank the Swedish Natural Science Research Council (NFR) for their financial support.

References

Aaronson, M., Tully, R. B., Fisher, J. R. et al., 1982, ApJS 50, 241
Bosma A., 1978, Ph.D. Thesis, University of Groningen
Bosma A., 1981, AJ 86, 1825
Bothun G.D., 1984, ApJ 277, 532
Bottinelli L., 1971, A&A 10, 437
Broeils A.H., 1992, Ph.D. Thesis, University of Groningen
Broeils A.H., van Woerden H., 1994, A&AS 107, 129 (Paper I)
Carignan C, Freeman K.C., 1985, ApJ 294, 949
Cayatte V., Kotanyi C., Balkowski C., van Gorkom J.H., 1994, AJ 107, 1003
Côté S., Carignan C., Sancisi R., 1991, AJ 102, 904
de Blok, W.J.G., McGaugh, S.S., van der Hulst, J.M., 1996, MNRAS, 283, 18
de Vaucouleurs G., de Vaucouleurs A., Corwin Jr. H.G., 1976, Second Reference Catalogue of Bright Galaxies, University of Texas Press, Austin
Faber S.M., Gallagher J.S., 1979, ARA&A 17, 135
Giovanelli R., Haynes M.P., 1983, AJ 88, 881
Han M., 1995, ApJ 442, 504
Huchtmeier A.L., Richter O.-G., 1988, A&A 203, 237
Kamphuis, J.J., Sijbring, D., van Albada, T.S., 1996, A&AS, 116, 15
Lake G., Schommer R.A., van Gorkom J.H., 1990, AJ 99, 547
Murtagh F., Heck A., 1987, Multivariate Data Analysis. Reidel, Dordrecht
Nilson, P., 1973, Uppsala General Catalogue of Galaxies, Nova Acta Regiae Soc. Sci. Upsaliensis, Ser. V:A, 1 (UGC)
Rhee M.-H., van Albada T.S., 1996, A&AS 115, 407 (Paper II)
Rhee M.-H., Broeils A. H., 1996, A&A, submitted
Roberts M.S., 1969, AJ 74, 859
Roberts M.S., Haynes M.P., 1994, ARA&A 32, 115 (RH)
Sancisi R., 1983, in Athanassoula E. ed, Internal kinematics and dynamics of galaxies. Reidel, Dordrecht, p.55
Shostak G.S., 1978, A&A 68, 321
Tormen G., Burstein D., 1995, ApJS 96, 123
Tully R.B., Fouqué P., 1985, ApJS 58, 67 (TFq)
van Driel W., 1987, Ph.D. Thesis, University of Groningen
Warmels R.H., 1986, Ph.D. Thesis, University of Groningen
Wevers B.H.M.R., 1984, Ph.D. Thesis, University of Groningen
Whitmore B.C., 1984, ApJ 278, 61

This article was processed by the author using Springer-Verlag LaTeX A&A style file *L-AA* version 3.